Matthew J. Emes, Maziar Arjomandi, Richard M. Kelso and Farzin Ghanadi

Turbulence length scales in a low-roughness near-neutral atmospheric surface layer

Journal of Turbulence, 2019; 20(9):545-562

Turbulence length scales in a low-roughness near-neutral atmospheric surface layer

Matthew J. Emes*, Maziar Arjomandi, Richard M. Kelso, Farzin Ghanadi

School of Mechanical Engineering, The University of Adelaide, SA, Australia

*Corresponding author. Email: matthew.emes@adelaide.edu.au

Turbulence length scales in a low-roughness near-neutral atmospheric surface layer

This paper investigated the integral length scales of turbulence in a low-roughness atmospheric surface layer (ASL), characterised by very smooth terrain in the Utah desert during near-neutral conditions, and evaluated the Engineering Sciences Data Unit (ESDU) 85020 and 86010 predictions for the turbulence length scales in a low-roughness ASL. The correlation integral method was used to estimate the integral length scales of the velocity components with longitudinal, lateral and vertical separations from sonic measurements on a vertical tower and spanwise array in the Surface Layer Turbulence and Environmental Science Test (SLTEST) field experiment. It was found that the longitudinal integral length scales calculated using near-neutral SLTEST data followed a logarithmic relationship with height proportional to the mean velocity profile with approximately constant integral time scale, however the sizes of the longitudinal components of the energy-containing eddies in the low-roughness flat terrain were 2-3 times smaller than those previously measured during field experiments in open country terrains. The calculated length scales with longitudinal separations over the very smooth terrain characteristics of the salt flats at Dugway were not consistent with those predicted by ESDU 85020. In contrast, the scaling of the lateral and vertical components of the three-dimensional turbulence structure with respect to the longitudinal component in the low-roughness ASL were consistent with similarity theory predictions in ESDU 86010 that the scaling ratios are independent of terrain roughness. Furthermore, this confirms the large dependence of the longitudinal turbulence length scales on the upstream terrain roughness and highlights the large variation of turbulence length scales observed at different low-roughness sites in the literature.

Keywords: integral length scale; integral time scale; cross-correlation; turbulence intensity; atmospheric surface layer

1. Introduction

Wind codes and standards for permanent physical structures, such as low- to medium-rise buildings, adopt a simplified gust factor approach that assumes quasi-steady wind loads based on a maximum gust wind speed. This can lead to significant errors for very tall buildings in urban terrains and stowed heliostat mirrors aligned parallel to the ground in desert terrains, due to their large dynamic responses to the large amplitude fluctuations during high-wind events such as gusts over short time intervals [1, 2]. Gusts are a rapid fluctuation of the instantaneous wind velocity from the mean wind over a specified sampling duration [3]. These flow fluctuations arise from eddies of varying sizes within the atmospheric boundary layer (ABL). The presence of "very large scale motions (VLSMs)" comprising packets of hairpin eddies with meandering regions of highly-elongated negative and positive velocity fluctuations have been observed in the outer boundary-layer that scale on the boundary-layer thickness δ [4, 5, 6] and contribute up to 60% of the total turbulent kinetic energy [7]. Although the combination of the "top-down" and "bottom-up" instability mechanisms responsible for generating these large-scale longitudinal eddy structures is unclear, they are impressed on the atmospheric surface layer (ASL), nominally the lowest 100 m of the ABL, as quasi-horizontal eddies but contribute little to the turbulent shear stress generated by surface-layer eddies produced by surface roughness and obstacles on the ground [6]. The average sizes of the energy-containing eddies in the longitudinal direction of the lower surface layer can be represented by the Eulerian integral length scale L_u^x, following Taylor's hypothesis that the turbulent flow field is translated downstream with uniform horizontal velocity U in the longitudinal direction. The magnitude of L_u^x relative to the characteristic length of a physical structure has a significant effect on the fluctuating pressures and unsteady forces on physical structures [8, 9], which can result in galloping and torsional flutter when the turbulence length scales and characteristic length scale of the physical structure are the same order of magnitude [10]. Small eddies result in wind loads on various parts of a structure that become uncorrelated with distance of separation, however large eddies whose size is comparable with the structure result in well correlated pressures over its surface as the eddy engulfs the structure, leading to maximum wind loads [1, 11]. Tall or slender structures with low natural frequencies are most likely to respond to the dynamic effects of gusts, which can lead to failure from excessive deflections and stresses due to flutter and random turbulent buffeting in the direction of the wind [1, 12]. Maximum wind loads at lower heights in the ABL will therefore tend to occur from the interaction of the largest eddies in the flow with a structure. Holdø, Houghton [13] found that the mean drag coefficient on the surface of a scale-model low-rise building of height D increased by 7% with an approximate doubling of L_u^x/D from 0.9 to 1.7 in a non-turbulent unsheared flow ($I_u = 2\%$), compared to a 46% increase as L_u^x/D increases from 1.6 to 3.6 in a turbulent sheared flow ($I_u = 25\%$ at $z/\delta = 0.2$) in the ABL simulated in a wind tunnel. Hence, consideration of the size of the largest eddies in the ABL relative to the characteristic length of a physical structure can lead to significant savings in costs due to the reduced design wind loading.

Turbulent motions in the near-neutral surface layer generated by surface roughness that are observed as wind velocity fluctuations (gusts) can be closely represented by the turbulence profiles of a zero-pressure gradient turbulent boundary layer [14]. The surface layer has been shown to have similar turbulence properties as the canonical turbulent boundary layer along a flat plate in a wind tunnel [15], such as a logarithmic velocity profile in the logarithmic region of the ASL consistent with scaling laws based on the attached eddy model [4, 16]. The near-wall turbulence within the lowest one-third of the neutrally-stratified ASL scales similarly to wall-bounded turbulence observed in the laboratory at lower Reynolds numbers, however the vertical turbulence intensities and eddy structures exhibit sharp increases further from the wall in the logarithmic region that deviate from classical scaling law and laboratory data [16]. In the lower region of the near-neutral ASL characterised by strong shear with eddy wavelengths larger than the observation height ($\lambda/z > 1$), Mikkelsen, Larsen [17] showed that the longitudinal turbulence spectra observed at Høvsøre for $z <$ 20-40 m were most accurately modelled by the Kaimal spectrum with an additional shear production subrange $\sim u_*^2 k^{-1}$ based on the friction velocity u_* and measurement height z. Hence, the first objective of this study is to compare laboratory profiles within a turbulent boundary layer to the turbulence intensity and Reynolds shear stress profiles calculated from the analysis of Surface Layer Turbulence and Environmental Science Test (SLTEST) velocity measurements [4, 18, 19, 20, 21] close to the ground in the Utah desert during selected near-neutral conditions.

Experimental field measurements in open country terrains have led to similarity theories concerning the spatial structure of turbulence in the surface layer. Semi-empirical models developed on the basis of similarity theory describe the flow over rural and urban terrains sufficiently to predict the surface shear stress, roughness height and turbulence intensities in the surface layer [22]. However, field measurements in rural terrains have shown considerable variation of integral length scales using different techniques. Teunissen [22] found that the correlation-integral approach using the autocorrelation function of velocity produced the largest longitudinal integral length scales in reasonable agreement with the Engineering Sciences Data Unit (ESDU 1974) model but only half those predicted by the model of Counihan [23]. Flay and Stevenson [24] suggested that the spectral-fit approach tended to underestimate length scales due to uncertainties associated with the identification of the peak in the broad spectra of slowly-varying turbulent eddies. Turbulent power spectra observations in the ASL have suggested that only the deviations of mean velocities, turbulence variances and length scales of the vertical component show consistent Obukhov scaling from site to site because of the absence of low-frequency components [25, 26]. In contrast, the low-frequency components of longitudinal turbulence cannot be consistently scaled from site to site because they are ‘very substantially enhanced by the “memory” of upstream terrain’ [26]. As a result, variation of the surface roughness height in open country and rural terrain ABLs has a significant effect on the distribution of longitudinal integral length scales at lower heights in the surface layer. The large variations in longitudinal turbulence length scales shown by field measurements [23, 24] at different sites and predicted by semi-empirical models, such as ESDU 85020 [27] and ESDU 86010 [28]. The inconsistent scaling of the low-frequency horizontal components of turbulence from site to site is caused by eddy-ground interactions within the “eddy shear layer” from differences in the upstream terrain with aerodynamic roughness height z_0 [6, 26]. However, similarity theory formulations derived in ESDU 86010 [28] predict that the spatial correlations of the lateral and vertical turbulence components are strongly correlated to the longitudinal turbulence component. Hence, the second objective of this study is to characterise the integral length scales of the three velocity components in a low-roughness ASL, using SLTEST field measurements obtained from Hutchins, Chauhan [4], for comparison with the integral length scales measured in rural terrains and predicted through autocorrelation and cross-correlation techniques by semi-empirical models in a low-roughness ASL.

The overall aim of this paper is to estimate the sizes and frequencies of the energy-containing turbulent eddies in a low-roughness surface layer using SLTEST field experiment measurements [4, 18, 19, 20, 21] in Dugway during near-neutral stability conditions for comparison with widely accepted semi-empirical models developed from similarity theory and experimental data. The sizes of the energy-containing eddies in the surface layer of the field experiment ABL [4] are estimated using autocorrelation and cross-correlation techniques to evaluate the integral length scales predicted by similarity theory correlations in ESDU 85020 [27] for longitudinal separations and ESDU 86010 [28] for lateral and vertical separations. The findings can be used to provide recommendations for improving the accuracy and versatility of the current methods used for calculating the turbulence length scales during near-neutral conditions in a low-roughness ASL.

2. Atmospheric Surface Layer Turbulence Theory and Methods

For the design of physical structures such as buildings with height D less than 100 m corresponding to the surface layer in Figure 1, the logarithmic law is most appropriate for modelling the mean longitudinal velocity profile $U(z)$ under the assumption of asymptotic similarity in a neutral ABL [29]

$$U(z) = \frac{u_*}{k} \ln\left(\frac{z}{z_0}\right) \quad (1)$$

Here u_* (m s^{-1}) is the friction velocity representing the Reynolds shear stress $\tau_s = -\rho u_*^2$ at the surface, k is von Karman's constant (here taken as 0.41) and z_0 (m) is the aerodynamic surface roughness height of the terrain, which can vary in scale from millimetres in a flat desert to metres in a dense urban area [30]. The design wind speed at the height of a physical structure in the ABL is normally calculated from measured gust velocities at the standard specification height of 10 m [27, 31, 32]. Hence, mean wind speeds are typically scaled to a 10 m reference height for the calculation of turbulence intensities, $I_i(z) = \sigma_i(z)/U(z)$, where σ_i (m s^{-1}) is the standard deviation of the fluctuating component of the instantaneous velocities $i = (u, v, w)$ in the streamwise (x), spanwise (y) and vertical (z) directions, respectively. Alternatively, viscous-scaled turbulence intensities are calculated as σ_i/u_* in the atmospheric surface layer (ASL) with respect to the friction velocity. Turbulence parameters are not measured routinely at most locations, so they must be estimated using similarity theory, the wind speed at the standard specification height of 10 m in the ASL, an estimated surface roughness length, and experimentally derived factors.

Similarity theory predicts that the sizes of the largest eddies are most dependent on the surface roughness height z_0 in the lower surface layer and on the boundary-layer thickness δ in the outer layer of the ABL [27]. The boundary-layer thickness δ cannot be directly measured in field experiments, however it is usually defined as the height where the mean gradient of the horizontal wind velocity is close to zero [33]. Following the Ekman solution that friction reduces the boundary layer wind speed below geostrophic (Figure 1), the depth of a neutral boundary layer can be estimated as [33]

$$\delta = 2ck\pi^2 \left(\frac{u_*}{f}\right) \ , \tag{2}$$

where c is a constant of proportionality equal to about 0.1 and $f = 2\omega \sin|\lambda| = 9.5 \times 10^{-5}$ rad/s is the Coriolis force at the latitude ($\lambda = 40.8°$ N) of the Bonneville salt flats in western Utah. The magnitude of δ varies diurnally between 100 m and 3 km with changes in atmospheric stability [33]. Wilson [19] showed that peak values of the ABL depth calculated from an idealised heat budget at the SLTEST site in Dugway increased to over 1 km during daytime hours.

The average thickness of the ABL in a neutral state with height-independent potential temperature is estimated to be of the order of $\delta \approx 600$ m, based on the analysis of data for high wind speeds ($U_{10\ \mathrm{m}} >$ 5-7 m s^{-1}) that produce adiabatic conditions [23]. It is noted that the ABL is only rarely in a neutral state, except in geographic locations that are subject to frequent strong winds. According to the Monin-Obukhov similarity theory, the influence of stratification on the state of the atmospheric surface layer is measured by the stability parameter defined as

$$\frac{z}{L} = \frac{g}{\theta_0}\frac{kz\overline{w'\theta'}}{-u_*^3} \,, \tag{3}$$

where g (m s^{-2}) is the gravitational acceleration, k is von Karman's constant, u_* (m s^{-1}) is the friction velocity calculated as $\left(\overline{u'w'}^2 + \overline{v'w'}^2\right)^{1/4}$ [33] in the current study at the reference height $z = 2.14$ m of the spanwise array, $\overline{w'\theta'}$ (m s^{-1} K) is the surface heat flux and θ_0 (K) is the mean temperature. Near-neutral stability in the inertial sublayer of the ASL during adiabatic conditions with a near-zero vertical heat flux $\overline{w'\theta'} \approx 0$ is commonly defined using the Högström [34] criterion that $|z/L| \leq 0.1$. The near-neutral surface layer thickness, denoted by δ_s in Figure 1, is considered by Hutchins, Chauhan [4] and Metzger, McKeon [14] as an effective boundary-layer thickness for the purposes of comparing with laboratory data of a turbulent boundary layer along a flat plate. The current study adopts the definition by Metzger, McKeon [14] that δ_s is approximated by the height at which the gradient of the horizontal velocity profile reaches a minimum during neutral conditions. This is a similar definition to the boundary layer thickness $\delta = z(U = 0.99U_\infty)$ along a flat plate in a wind tunnel, thus allowing reasonable comparison of non-dimensional heights in atmospheric and laboratory turbulent boundary layers.

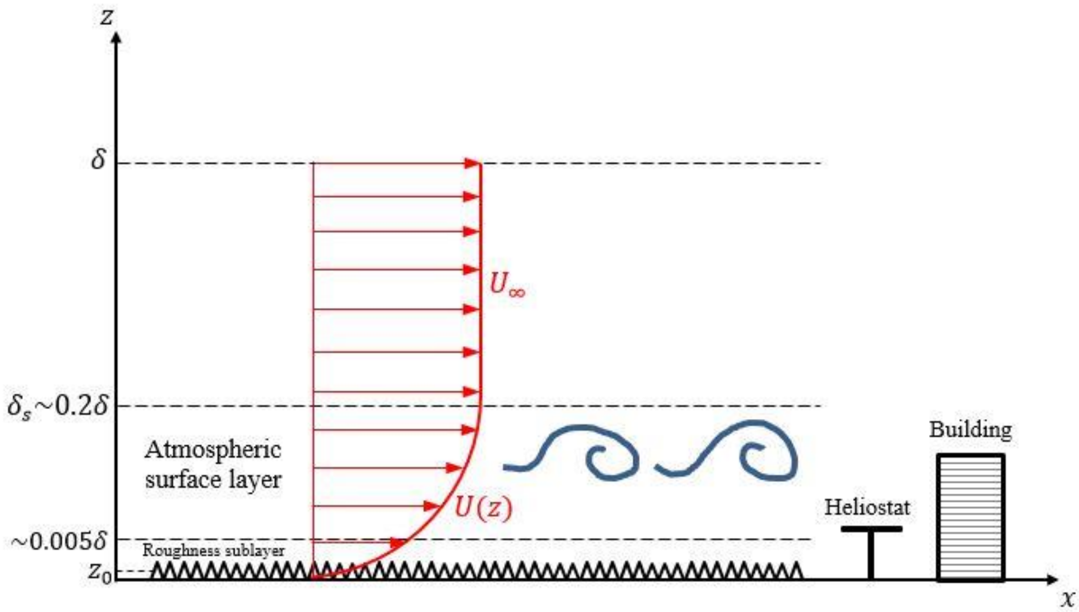

Figure 1. Turbulence characteristics and structure of the atmospheric surface layer.

The longitudinal integral length scale L_u^x (m) at a given height z is calculated from the tranformation of point velocity measurements as a function of time to spatially distributed data by Taylor's hypothesis. This assumes that eddies are embedded in a frozen turbulence field convected downstream at the mean wind speed U (m s^{-1}) in the streamwise direction $\Delta x = U\Delta t$, and hence do not evolve with time t [35]. The integral length scale of the velocity component $i = (u, v, w)$ at a given height z in the ASL is therefore calculated as [36]

$$L_i^x(z) = T_i^x(z)U(z), \tag{4}$$

where T_i^x (s) is the integral time scale of the fluctuating velocity component i, representing the time taken for the average sizes of the energy-containing eddies to traverse a single point in the longitudinal x direction. The integral time scale is calculated using Equation (6) by the integral of the autocorrelation function $R_i(\tau)$ in Equation (5) to its first-zero crossing τ_0, assuming that $R_i(\tau)$ fluctuates close to zero after this point [36]. When the autocorrelation curve decreases rapidly to zero, the peak value of the power spectrum is shifted to higher frequencies. The transfer of kinetic energy by the stretching and distortion of larger eddies to smaller eddies becomes excessively large in the high-frequency region of the spectrum, which leads to dissipation by viscosity at the Kolmogorov length scale [37].

$$R_i(\tau) = \frac{\overline{\iota'(t)\iota'(t+\tau)}}{{\sigma_i}^2}, \tag{5}$$

$$T_i^x = \int_0^\infty R_i(\tau)\, d\tau \approx \int_0^{\tau_0} R_i(\tau)\, d\tau. \tag{6}$$

Here $i = (u, v, w)$ defines the velocity components in the longitudinal direction. Cross-correlation of the velocity component i between two points with separation distances Δy in the lateral direction or Δz in the vertical direction are calculated as follows:

$$R_{ii}(\Delta j, \tau = 0) = \frac{\overline{\iota'(j)\iota'(j+\Delta j)}}{\sigma_i(j)\sigma_i(j+\Delta j)}, \tag{7}$$

$$T_i^j = \int_{\Delta j=0}^{\Delta j_{max}} R_{ii}(\Delta j)\, d\Delta j. \tag{8}$$

The majority of integral length scale data available in the literature has been obtained from field-site anemometer velocity measurements in rural and urban ABLs [22, 23, 24], from which several semi-empirical equations have been derived to estimate the length scale profiles in the neutral ASL as a function of the aerodynamic surface roughness height of the terrain. ESDU 85020 [27] is a dataset based on a semi-empirical model for integral length scales of atmospheric turbulence over uniform terrain in a neutral ABL based on a reference mean wind speed $U_{10r} = 20$ m s^{-1} at a 10 m height over open country terrain (z_0 = 30 mm) with f = 1 × 10^{-5} rad s^{-1} [27]. A correction factor k_L is provided to account for the variation of L_u^x with changes in U_{10r} and f within an estimated ±8% error [27]. The model of Counihan [23] predicts the variation of longitudinal integral length scale with height as

$$L_u^x(z) = Cz^{1/n}, \tag{9}$$

where C and $1/n$ are empirical variables as a function of the roughness height z_0. Solari and Piccardo [38] proposed the following equation ($z \leq 200$ m) based on the analysis of integral length scale data in terrains with surface roughness height z_0 ranging from 10 mm to 1 m:

$$L_u^x(z) = 300\left(\frac{z}{200}\right)^{0.67+0.05\ln(z_0)}. \tag{10}$$

AS/NZS 1170.2 uses the following formula to predict the integral length scale in the ABL for the design of low- to medium-rise buildings ($z \leq 200$ m)

$$L_u^x(z) = 85\left(\frac{z}{10}\right)^{0.25}. \tag{11}$$

3. Experimental Facility and Data Pre-treatment

Turbulence characteristics in the atmospheric surface layer (ASL) that develop from a shear-driven wall-bounded flow can be most simply and independently assessed from thermal effects during neutral conditions at high wind speeds that form the basis of wind codes and standards. Measurements of wind velocity were acquired from a field experiment study carried out by a large team comprising individuals from the University of Utah, University of Edinburgh, University of Minnesota, University of Melbourne, Imperial College, London, and the University of Alberta at the Surface Layer Turbulence and Environmental Science Test (SLTEST) facility in the western Utah Great Salt Lake desert. The unique geography of the site enabled measurements to be taken in a very high Reynolds number ABL ($Re_* = \delta u_*/\nu \approx 6\times10^5$) that has developed over 100 km of low surface roughness salt flats to the north of the SLTEST facility in Dugway Proving Grounds, Utah [5, 20, 21, 40]. Raw temperature and velocity data were measured simultaneously at the SLTEST site for approximately 6 days from 27 May to 3 June 2005 using nine three-dimensional Campbell Scientific (CSAT3) sonic anemometers in a vertical tower array at heights $z =$ (1.42, 2.14, 3.00, 4.26, 6.14, 8.71, 12.52, 17.94 and 25.69) m and a spanwise array of ten CSAT3 anemometers at $z = 2.14$ m separated by equal distances of 3 m to the west of the vertical tower [18]. Three components of velocity in the streamwise x, spanwise y and vertical z directions were collected at a sampling frequency of 20 Hz [4]. All of the anemometers were oriented for predominantly uniform winds from the nominal north at an azimuth angle $\alpha = 0°$ [18, 20]. It was noted by Wilson [19] that the tower had been installed near a raised parking area, on which stood several large instrument trailers. This caused some flow distortion at heights below 6.14 m in the vertical array, such as a 6% reduction in mean wind speed recorded by the tower sonic at $z = 3$ m compared with anemometers at the same height in a horizontal array positioned at least 10 m west of the tower [21]. Despite this mean velocity discrepancy, comparisons of spectra at the nine heights in the vertical array by McNaughton, Clement [21] showed an insignificant effect of the disturbed flow by the downwind obstacles.

Conditions of neutral stability with negligible buoyancy effects were required to effectively compare statistically stationary data from canonical laboratory turbulent boundary layers [14, 41]. For neutrality of the SLTEST dataset, Hutchins, Chauhan [4] used the criterion of Högström [34] that $|z/L| \leq 0.1$, which has been used in the current study. Table 1 shows ten hours in local time (LT = UTC – 6 h) that satisfy the following selection criteria for "near-neutral" conditions at the reference height $z = 2.14$ m on the vertical SLTEST tower: stability parameter $|z/L| \leq 0.1$, friction velocity $u_* \geq 0.15$ m s^{-1}, and steady winds with mean streamwise velocity $U \geq 5$ m s^{-1} and a mean flow angle $|\alpha| = \tan^{-1}(V/U) \leq 20°$ within the angular response of the sonic anemometers to ensure that the flow was well-aligned with respect to the anemometers for an accurate estimate of the shear stresses (friction velocities) and integral length scales. The raw horizontal velocity components u in the longitudinal direction and v in the lateral direction were corrected using trigonometric equations and the mean wind direction.

Following the wind direction adjustment, the method introduced by Hutchins, Chauhan [4] for de-trending the velocity data was used to remove the long-term weather trends to obtain the turbulent fluctuations of the shear-generated flow associated with the average length scales of eddies in the lowest third of the atmospheric surface layer [17, 42]. A low-pass filter corresponding to a wavelength of 20δ for an estimated surface layer thickness $\delta = 100$ m is applied to the velocity fluctuations derived from the corrected longitudinal velocity component. This large-scale synoptic wave is removed from the fluctuating velocity signal to obtain the turbulent velocity fluctuations for analysis and comparison of the turbulence intensities and integral length scales with laboratory data and semi-empirical models, such as ESDU 85020 [27] based on similarity theory.

The wall-normal heat flux $\overline{w'\theta'}$ remained close to zero during the ten selected near-dawn hours, hence the effects of buoyancy and non-stationarity from the transition in the sign of the heat flux can be considered negligible relative to the shear-generated turbulence in a neutral ASL [4]. The streamwise mean wind speed U is 8 m s^{-1} at a 2.14-m height during near-neutral hour 6 in Table 1, which was shown by Hutchins, Chauhan [4] to closely approximate the mean velocity statistics of a laboratory turbulent boundary layer along a flat plate. Velocity data from the ten near-neutral hours selected in Table 1 were used for analysis of the turbulence profiles and statistics in Section 4. The calculation of integral length scales of the fluctuating velocity components were averaged over the ten near-neutral hours in Table 1 in order to present the statistical variability in the data.

Near-neutral hour	Date 2005	Time LT	Stability parameter z/L	Friction velocity u_* (m s^{-1})	Mean streamwise velocity U (m s^{-1})	Mean flow angle α (°)
1	27 May	0500-0600	0.06	0.15	4.9	-6.9
2	1 June	0600-0700	0	0.42	5.1	-10.5
3	1 June	0700-0800	0	0.47	4.9	-10.1
4	1 June	0800-0900	0.002	0.30	5.8	-5.6
5	1 June	0900-1000	0.001	0.28	5.3	-1.8
6	2 June	0400-0500	0.01	0.25	8.0	-12.9
7	2 June	0500-0600	-0.01	0.36	9.1	4.4
8	2 June	0600-0700	-0.002	0.31	8.1	12.4
9	2 June	0700-0800	-0.008	0.29	7.4	-14.4
10	2 June	0800-0900	0	0.20	5.4	-15.7

Table 1. Mean velocities and flow angles of SLTEST velocity data at $z = 2.14$ m for selected near-neutral hours ($|z/L| \leq 0.1$).

The nine sonic anemometers in the wall-normal array were logarithmically spaced at heights between 1.42 m and 25.69 m. The measurement heights in the SLTEST field experiment were scaled on a near-neutral surface layer thickness δ_s of 80 ± 8 m, estimated from the height at which the mean velocity gradient of the horizontal wind reaches a minimum using prior radiosonde measurements acquired near sunset [14]. Hutchins, Chauhan [4] estimated that $\delta_s \approx 60$ m for a one-hour period (near-neutral hour 6 in Table 1) from a composite best-fit of $\overline{u'u'}/u_*^2$ and $-\overline{u'w'}/u_*^2$ with laboratory data of a zero-pressure-gradient turbulent boundary layer. It is noted that these techniques introduce some experimental uncertainties in the estimation of δ_s compared to an independent measurement of the wall shear stress. The boundary-layer thickness δ during the near-neutral hours in Table 1 is estimated to be of the order of 1000 m using Equation (3), with similar magnitudes to those inferred by Wilson [19] using an idealised heat budget. Since δ and δ_s could not be directly calculated from the SLTEST measurements due to the maximum measurement height of 25.69 m on the vertical tower, there is an uncertainty of at least 10% in their estimated values.

In the current study, laboratory data were used for comparison to demonstrate the similarities of turbulence intensities and Reynolds stresses near the ground in the neutral ASL and along a flat plate in a zero-pressure-gradient turbulent boundary layer. This would allow the SLTEST surface layer to be compared with the logarithmic law mean velocity profile and turbulence intensity profiles that have been non-dimensionalised with the boundary-layer thickness on a flat plate in a wind tunnel.

4. Results

Figure 2 shows the mean streamwise velocity profile, normalised with respect to the friction velocity and averaged over the ten near-neutral hours in Table 1, compared with the non-dimensional form of the logarithmic profile in Equation (1). The error bars on the SLTEST mean velocity profile indicate one standard deviation from the mean value of the ten near-neutral hours. The SLTEST mean velocity profile in Figure 2 is most closely represented by a logarithmic profile with an aerodynamic roughness height $z_0 \approx 2$ mm, in agreement with the finding by Kunkel and Marusic [43] that the terrain over the salt flats in Dugway was best approximated as a mildly transitional rough surface with an equivalent sand-grain roughness height $k_s^+ \approx 21$. It is noted that the maximum difference between the SLTEST and logarithmic profiles is less than 1% at $z \geq 8.71$ m, whereas this difference is 2-5% at $z \leq 6.14$ m due to the flow interference by the nearby field trailers [19, 21]. Hence, the SLTEST mean velocity profiles suggest that the desert surface in Dugway Proving Grounds, Utah can be characterised as a low-roughness turbulent boundary layer along a flat plate.

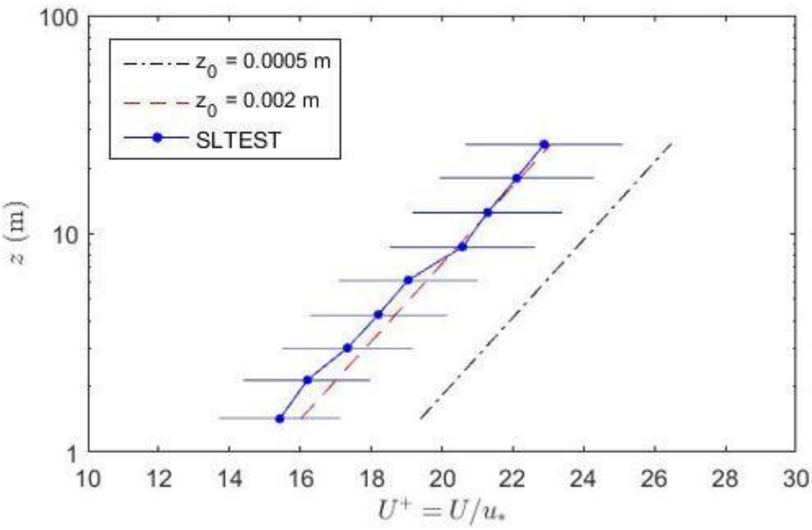

Figure 2. Mean velocity profile $U^+ = U/u_*$ normalised with friction velocity of the SLTEST data and averaged over the 10 near-neutral hours in Table 1, compared with theoretical models for a logarithmic velocity profile U/u_* in the non-dimensional form of Equation (1) with $z_0 = 0.0005$ m and 0.002 m. Error bars on the SLTEST mean velocity profile indicate one standard deviation from the mean value.

Figure 3(a,b) present the turbulence intensity profiles of the SLTEST data during near-neutral hour 6 in the streamwise and spanwise directions with a maximum 10% experimental error in the estimate of the friction velocity $u_* = 0.25$ m s^{-1}. The height is non-dimensionalised with respect to an estimated surface layer thickness δ_s = 100 m in the SLTEST field experiment for a least-squares fitting of the streamwise turbulence intensity σ_u/u_* profile within ±10% of smooth and rough wall laboratory data from Hinze [44] in a zero-pressure-gradient turbulent boundary layer. In contrast, the spanwise turbulence intensity profile σ_v/u_* deviates by more than 10% from the rough wall turbulent boundary layer at $z/\delta_s > 0.2$. A least-squares fit of the spanwise turbulence fluctuations in the SLTEST data to the laboratory data showed that the surface layer thickness is closer to the estimate by Hutchins, Chauhan [4] of δ_s = 60 m during near-neutral hour 6. There is a large uncertainty in these estimates of δ_s, as the largest anemometer height of 25.69 m on the vertical tower array in the SLTEST measurements was less than half that of the predicted δ_s where the gradient of the horizontal wind speed approaches zero. The estimate of $\delta_s = 80$ ± 8 m by Metzger, McKeon [14], determined using horizontal velocity and temperature profiles acquired from a tethersonde near sunset during near-neutral conditions at heights of up to 300 m at the SLTEST site, is therefore considered a feasible approximation for each of the ten near-neutral hours in Table 1. Although the Reynolds number, $Re_* = \delta_s u_*/\nu$ =$7.9\times10^5 - 2.5\times10^6$ for $\delta_s = 80$ m and u_* in Table 1, is an order of magnitude larger in the SLTEST field experiment, the turbulence intensity profiles show good agreement with laboratory data for a smooth wall within the estimated experimental error of the friction velocity in the SLTEST data. Furthermore, the profile of the Reynolds shear stresses averaged over the ten near-neutral hours in Figure 3(c) is in close agreement with the profile calculated by Hutchins, Chauhan [4] during near-neutral hour 6. The Reynolds stress profile as a function of the inner-scaled viscous height $z^+ = zu_*/\nu$ in the current study is also consistent with the theoretical prediction curve of Chauhan [45] following similarity formulations for a wall-bounded turbulent boundary layer. This provides further validation that the turbulence statistics in the near-neutral ASL are as predicted from laboratory-based studies of flat-plate turbulent boundary layers.

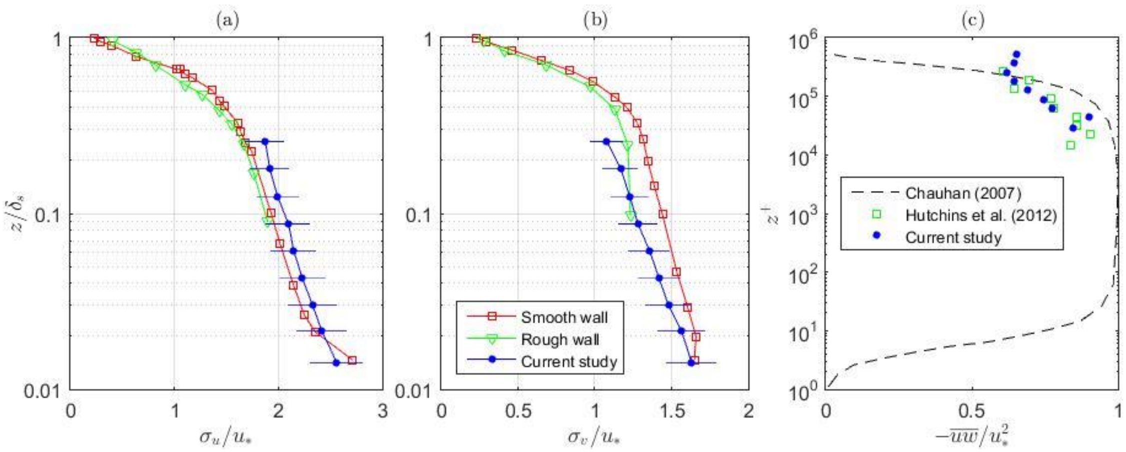

Figure 3. (a) Streamwise turbulence intensity, (b) Spanwise turbulence intensity profiles during near neutral hour 6 (0400 – 0500 LT on 2 June 2005) of the SLTEST data as a function of non-dimensional height z/δ_s with an estimated surface layer thickness δ_s = 100 m. Error bars on the SLTEST data in (a) and (b) indicate a maximum 10% error in the estimate of friction velocity u_*. Smooth and rough wall data were taken from Hinze [44] for a zero-pressure-gradient turbulent boundary layer along a flat plate. The smooth wall has $u_*/U_\infty \approx 0.037$ and Re_* = 75,000 and the rough wall has $u_*/U_\infty \approx 0.055$ and Re_* = 67,000. (c) Reynolds stress profile averaged over the ten near-neutral hours in the current study compared with the profile calculated by Hutchins, Chauhan [4] during near-neutral hour 6. The dashed line represents the similarity formulation from Chauhan [45].

Figure 4(a) shows the autocorrelation function R_u of the streamwise velocity at three heights in the SLTEST field experiment for the largest mean wind speed ($U_{10\text{ m}} = 7.93$ m s^{-1}) of near-neutral hour 6. It is noted that R_u of the fluctuating velocity signal decreases quickly with time lag τ towards the first-zero crossing after τ = 20 s. The differences between the methods for estimating the integral length scales in Figure 4(b) highlights their sensitivity to time-scale filtering techniques applied to velocity measurements in micrometeorological studies. Approximating the shape of R_u by an exponential fit by integrating $R_u(\tau)$ to $1/e$ yielded longitudinal integral length scales L_u^x in Figure 4(b) that were 22% and 16% lower on average at the SLTEST measurement heights than the correlation integral and spectral fit methods, respectively. The integral length scales L_u^x in Figure 4(b) were also derived following the filtering method proposed by Salesky, Chamecki [46] using a power-law fit to the flux of the filtered velocity signal over a specified range of time filters to calculate the integral time scales. The length scales yielded by the correlation integral method were consistently larger than those calculated using the filtering and spectral fit methods at all of the SLTEST measurement heights, in agreement with the findings by Salesky, Chamecki [46]. The uncertainty in the spectral fit method may be explained by the difficulty in locating the peak of the power spectra over the relatively smooth terrain of the Utah desert. However, the large differences between the filtering method and the first-zero crossing correlation method are unclear but may be due to a poorly represented power-law fit to the standard deviation of the filtered velocity fluxes in the filtering method. Integrating under the $R_u(\tau)$ curve to the first-zero crossing τ_0 has been suggested by several experimental and numerical studies [36, 47, 48] to estimate the turbulence length scales within a turbulent boundary layer, which yielded similar results to integrating to $R_u(\tau) = 0.05$ in the current study. Hence, the correlation integral to the first-zero crossing was considered the most appropriate method because of clearly defined limits of integration, consistent fluctuation of R_u about zero after τ_0 and relatively smaller uncertainties compared to the other methods. It is observed that the profiles of L_u^x increase logarithmically with height following the mean wind velocity profile $U(z)$ in Figure 2. The integral time scales T_u^x and T_v^x in Figure 4(d) are approximately invariant with respect to the height within the ASL, which suggests that the power spectra of the horizontal velocity components are dominated by the inactive eddies during near-neutral conditions. Figure 4(e) shows the effect of atmospheric stability on the T_u^x profiles as a function of the stability parameter z/L calculated using Equation (3) from selected SLTEST data at the reference height $z = 2.14$ m on the vertical tower for selected individual hours with mean flow angle $|\alpha| \leq 20°$. It is observed that the integral time scales are relatively constant with height and increase with decreasing z/L from T_u^x =1.6 s during stable conditions ($z/L = 0.13$) to $T_u^x = 3.2$ s during near-neutral stratification ($z/L \approx 0$) and $T_u^x = 5.5$ s in the strongly unstable or convective ASL ($z/L =$ -2). However, the integral time scales averaged over multiple hours from additional data sets in low-roughness terrains within a similar stability range would provide representative values of T_u^x for different stability regimes.

Figure 4(c) shows the integral length scales of the three velocity components, averaged over the ten near-neutral hours in Table 1 with a maximum variation of ±30% from the mean values, using the correlation integral method as a function of height in the SLTEST surface layer. The ratios of the integral length scales for separations in the longitudinal direction are $L_u^x/L_v^x \approx 1.4$, $L_u^x/L_w^x \approx 27$ and $L_v^x/L_w^x \approx 20$. The corresponding ratios for isotropic turbulence are 2, 2 and 1, respectively, indicating the significant contribution of spectral power in the horizontal velocity components that reflects the large inactive eddies with scales nominally proportional to the boundary layer thickness. The ratio of L_u^x/z varies from 2 to 10 with decreasing height z from 25.69 m to 1.42 m on the vertical SLTEST tower in Figure 4(c), which suggests that small physical structures of height D in the surface layer of low-roughness terrains are exposed to sizes of the energy-containing eddies that are of the same order of magnitude as the characteristic dimension of the physical structure. These ratios have generally been found to result in the maximum wind loads due to turbulent buffeting [1, 11].

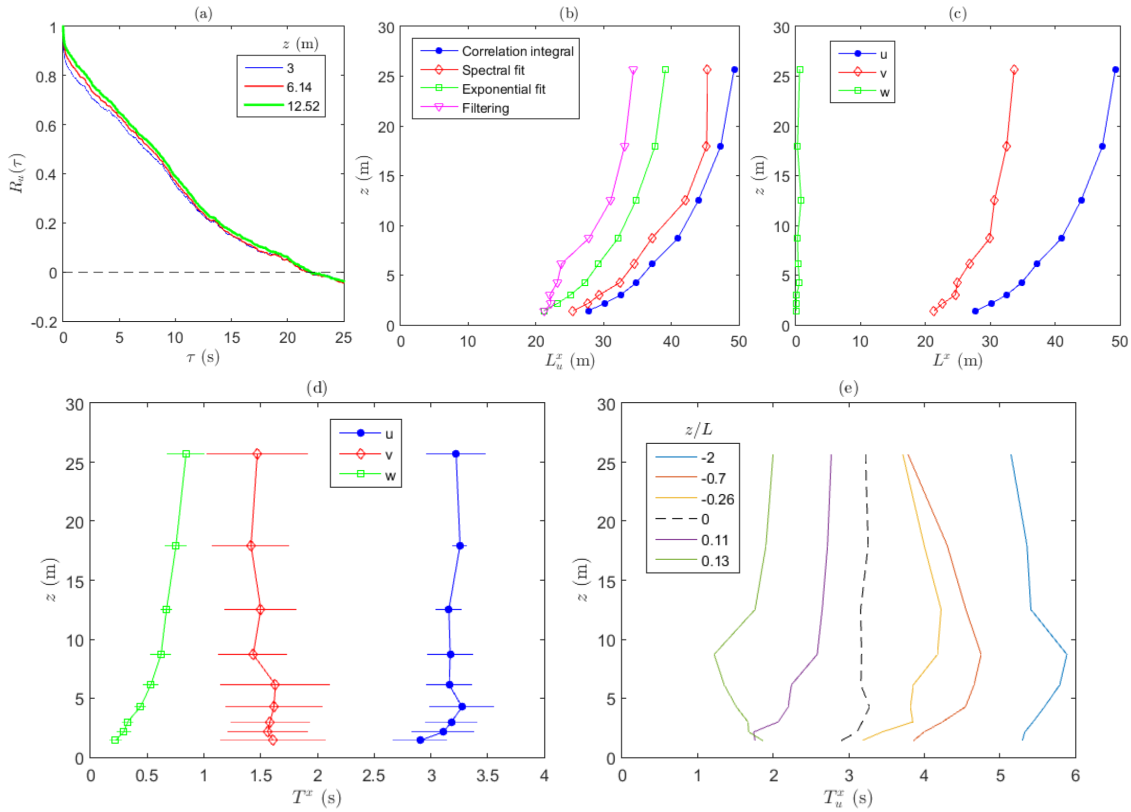

Figure 4. Distributions of integral length scales with height in the SLTEST field experiment: (a) Autocorrelation function of streamwise velocity as a function of time lag τ at three heights in the SLTEST surface layer during near-neutral hour 6 (0400 – 0500 LT on 2 June 2005); (b) Longitudinal integral length scales calculated during near-neutral hour 6 using four different methods: integral to the first-zero crossing of R_u, fitting of the von Karman equation to the turbulent spectra, exponential fit by integrating to $R_u = 1/e$, and the filtering method proposed by Salesky, Chamecki [46]; (c) Integral length scale profiles of the streamwise u, spanwise v and vertical w velocities for separations in the longitudinal x direction averaged for the 10 near-neutral hours selected in Table 1; (d) Integral time scale profiles of the three velocity components for separations in the longitudinal x direction. Error bars indicate one standard deviation from the mean value showing the variation between the near-neutral hours in Table 1; (e) Integral time scale profiles as a function of the stability parameter z/L based on individual hours of velocity data at the reference height $z = 2.14$ m on the vertical SLTEST tower for steady winds with mean flow angle $|\alpha| \leq 20°$. The dashed line for neutral stability ($z/L = 0$) is calculated from the average T_u^x over the ten near-neutral hours with standard deviation shown by the error bars in Figure 4(d).

Figure 5 presents the distribution of longitudinal integral length scales with height in the SLTEST surface layer, estimated using the correlation integral method in comparison with experimental measurements in low-roughness surface layers and semi-empirical equations. The logarithmic profile of L_u^x shown in Figure 4(c) is reflected in field measurements in open country terrains ($z_0 \approx 30$ mm), such as those reported by Flay and Stevenson [24] on short grassy plains near Christchurch. Integral length scale profiles predicted by ESDU 85020 [27] correlations were previously observed by Farell and Iyengar [49] to be an upper bound to field measurements in surface layers over open country and urban terrains. It is clear from Figure 5 that the L_u^x profiles predicted by the semi-empirical models [23, 27, 38] for a low-roughness terrain are not consistent with the L_u^x profile calculated using the SLTEST data during near-neutral conditions. This suggests that the estimation in semi-empirical models that L_u^x generally increases with decreasing z_0 at a constant height in the surface layer may not reliably approximate the case of a very low roughness terrain. However, it must be noted that the values of L_u^x from an extensive range of surface layer measurements reported by Counihan [23] vary by as much as an order of magnitude in the lowest 10 m over low-roughness terrains. The large variation in L_u^x at lower heights in surface layers is enhanced by differences in the upstream terrain and thus the low-frequency components of the horizontal components of turbulence cannot be consistently scaled from site to site [26].

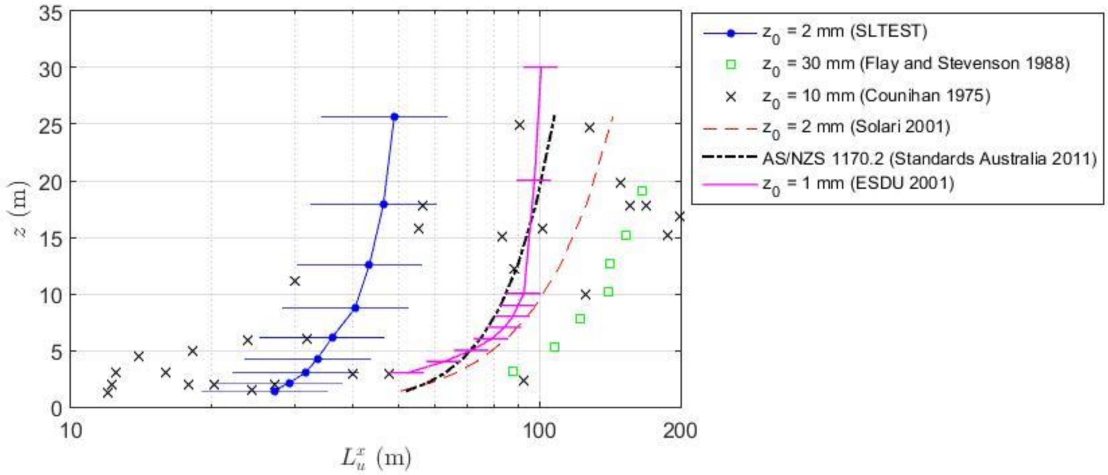

Figure 5. Longitudinal integral length scales calculated using the correlation integral method as a function of height in the SLTEST field experiment compared with those measured in low-roughness surface layers [23, 24] and predicted by semi-empirical equations [27, 32, 38]. Error bars on the SLTEST data indicate the average variation of ±30% of L_u^x observed during the ten near-neutral hours selected in Table 1. Error bars on the ESDU curve indicate a ±8% error in the variation of L_u^x with changes in mean wind speed.

Table 2 shows the longitudinal turbulence length scales calculated by autocorrelation and their ratio with the spanwise and vertical length scales at the standard reference height of 10 m. Length scales of the longitudinal velocity component varied from 27 m to 49 m in the height range of the SLTEST vertical tower during neutral conditions, however the average $L_u^x = 42$ m at the standard 10-m measurement height was not consistent with semi-empirical models and other field measurements. The average value of L_u^x during neutral hours is 2-3 times smaller than those measured over flat “open country” terrains [22, 24] and those predicted by ESDU 85020 [27] during neutral conditions with $U = 8.6$ m/s, $f = 9.5\times10^{-5}$ rad/s and $z_0 = 0.002$ m. The ratios L_v^x/L_u^x and L_w^x/L_u^x in the desert ASL are at least 15% and 35% larger than field measurements by Flay and Stevenson [24] and approximately double those by Teunissen [22]. This suggests that the upstream terrain has a greater effect on L_u^x than on L_w^x, which is in agreement with the findings of Panofsky, Larko [26]. However, Table 2 shows that the calculated L_u^x in the current study during neutral conditions are not consistent with ESDU 85020 [27] predictions in a low-roughness ASL. This may be due to the small data set limited by the measurement period and the constraints of data selection for steady wind conditions.

Length scales	**Current study**	**ESDU 85020 [27]**	**Teunissen [22]**	**Flay and Stevenson [24]**
L_u^x (m)	42	93	62	88
L_v^x/L_u^x	0.46	0.25	0.18	0.39
L_w^x/L_u^x	0.20	0.09	0.08	0.13

Table 2. Average ratios of turbulence length scales L_i^x of the neutral SLTEST velocity data in Table 1 at the standard reference height $z = 10$ m, compared with ESDU 85020 [27] and field measurements [22, 24].

Table 3 shows the cross-correlation turbulence length scales ratios, compared with those predicted by ESDU 86010 [28] and other field measurements [22, 24]. In contrast to the length scales with longitudinal separations in Table 2, the ratios of the longitudinal and vertical length scales with lateral and vertical separations to the longitudinal length scale, $L_u^y/L_u^x = 0.28$, $L_u^z/L_u^x = 0.32$, $L_w^y/L_u^x = 0.07$ and $L_w^z/L_u^x = 0.06$ showed good agreement with other field measurements. Hence, the scaling effects of the lateral and vertical turbulence components of the three-dimensional turbulence structure in a low-roughness ASL are consistent with similarity theory predictions. This suggests that the scaling of the three-dimensional spatial variation of turbulent energy-containing eddies during neutral conditions in the ASL is consistent and independent of terrain roughness.

Length scales	**Current study**	**ESDU 86010 [28]**	**Teunissen [22]**	**Flay and Stevenson [24]**
L_u^y/L_u^x	0.28	0.28	0.39	0.24
L_v^y/L_u^x	0.32	0.27	0.46	0.35
L_w^y/L_u^x	0.07	0.05	0.06	0.05
L_u^z/L_u^x	0.27	0.33	–	0.23
L_v^z/L_u^x	0.14	0.16	–	0.26
L_w^z/L_u^x	0.06	0.06	–	0.08

Table 3. Average ratios of turbulence length scales, L_i^y/L_u^x and L_i^z/L_u^x, calculated by cross-correlation of neutral SLTEST velocity data in Table 1 at the reference height $z = 2.14$ m ($L_u^x = 27$ m) for the spanwise array and $\bar{z} = 9$ m ($L_u^x = 40$ m) for the vertical tower, respectively. Comparison with ESDU 86010 [28] and field measurements [22, 24] at $z = 10$ m.

5. Conclusions

The turbulence length scales over a very flat, open terrain in a desert surface layer have been investigated based on ten hours of SLTEST velocity data measurements [4, 18, 19, 20, 21] during near-neutral conditions. The very small data set of ten near-neutral hours analysed is a limitation of the current study due to the constraints of data selection with a near-zero stability parameter, a sufficient horizontal wind speed and a mean flow angle that is not excessively large with respect to the orientation of the anemometers in the vertical array for an accurate estimate of the shear stresses and integral length scales. It is acknowledged that further studies and data sets in low-roughness terrains are required in order to verify and extend the findings. Nevertheless, the following major conclusions can be drawn:

- For the purposes of studying the turbulence length scales in a neutrally-stratified ABL, the mean velocity profile during the ten near-neutral hours of SLTEST data selected is consistent with the logarithmic profile of a low-roughness ($z_0 = 0.002$ m) terrain within a maximum error of 1% at $z \geq 8.71$ m and 5% at $z \leq 6.14$ m due to the flow interference by the nearby field trailers [19, 21]. Turbulence intensity and Reynolds stress profiles calculated from SLTEST data during near-neutral conditions show good agreement with laboratory data from Hinze [44] for a smooth wall when the height is non-dimensionalised with respect to an estimated surface layer thickness δ_s of 80 m. This is in agreement with radiosonde measurements by Metzger, McKeon [14] at heights up to 300 m and hence, provides further validation that the turbulence profiles in the near-neutral atmospheric surface layer are similar to those in the canonical turbulent boundary layer on a flat plate.

- Integral length scales calculated by the integration of the autocorrelation function of velocity R_u to the first-zero crossing τ_0 yielded the largest values of L_u^x and was considered the most appropriate method because of clearly defined integration limits, consistent fluctuation of R_u about zero after τ_0 and relatively smaller errors than locating the peak of the power spectra in the spectral fit method and approximating R_u as an exponential function. The horizontal velocity components in the longitudinal and lateral direction contribute a significant portion of the spectral power, which is associated with the large eddies that scale nominally on the boundary layer thickness. The integral time scales were found to be relatively independent of the measurement height in the SLTEST surface layer and increase with decreasing stability parameter z/L from T_u^x =1.6 s during mildly stable conditions (z/L = 0.13) to T_u^x = 3.2 s in the near-neutral ASL ($z/L \approx$ 0) and T_u^x = 5.5 s in the convective ASL (z/L = -2).
- The logarithmic variation of the longitudinal integral scale L_u^x with height at the SLTEST site is consistent with that predicted by semi-empirical models [23, 27, 38], however the average L_u^x = 42 m at a 10-m height during near-neutral conditions is 2-3 times smaller than those measured during field experiments in open country terrains. The smaller turbulence length scales are likely to be due to the very smooth terrain features of the salt flats at Dugway. Hence, the sizes of the horizontal velocity components of the energy-containing eddies with longitudinal separation distances in the lower region of the ASL are significantly dependent on the upstream terrain roughness. In contrast, the scaling of the lateral and vertical turbulence components with respect to the longitudinal component of the three-dimensional turbulence structure in a low-roughness ASL is consistent with similarity theory predictions. The ratios of the length scales with lateral and vertical separations to the longitudinal length scale, L_u^y/L_u^x = 0.28, L_u^z/L_u^x = 0.32, L_w^y/L_u^x = 0.07 and L_w^z/L_u^x = 0.06, showed good agreement with other field

measurements [22, 24] in open country terrains and ESDU 86010 [28], which suggests that the length scale ratios are independent of terrain roughness.

Acknowledgements

I acknowledge the support I have received for my research through the provision of an Australian Government Research Training Program Scholarship. Further support for the work has been provided by the Australian Solar Thermal Research Initiative (ASTRI), through funding provided by the Australian Renewable Energy Agency (ARENA). The authors also acknowledge Associate Professor Nicholas Hutchins and Dr Kapil Chauhan for their contribution of velocity data obtained from the SLTEST facility in Dugway, Utah, USA.

References

1. Mendis P, Ngo T, Haritos N, et al. Wind loading on tall buildings. EJSE Special Issue: Loading on Structures. 2007;3:41-54.
2. Durst CS. Wind speeds over short periods of time. Meteorological Magazine. 1960;89(1960):181-186.
3. Kristensen L, Casanova M, Courtney M, et al. In search of a gust definition. Boundary-Layer Meteorol. 1991;55(1-2):91-107.
4. Hutchins N, Chauhan K, Marusic I, et al. Towards reconciling the large-scale structure of turbulent boundary layers in the atmosphere and laboratory. Boundary-Layer Meteorology. 2012;145(2):273-306.
5. Hutchins N, Marusic I. Evidence of very long meandering features in the logarithmic region of turbulent boundary layers. Journal of Fluid Mechanics. 2007;579:1-28.
6. Hunt JC, Morrison JF. Eddy structure in turbulent boundary layers. European Journal of Mechanics-B/Fluids. 2000;19(5):673-694.
7. Wang G, Zheng X. Very large scale motions in the atmospheric surface layer: a field investigation. Journal of Fluid Mechanics. 2016;802:464-489.
8. Emes MJ, Arjomandi M, Ghanadi F, et al. Effect of turbulence characteristics in the atmospheric surface layer on the peak wind loads on heliostats in stow position. Solar Energy. 2017;157:284-297.
9. Pfahl A, Randt M, Meier F, et al. A holistic approach for low cost heliostat fields. Energy Procedia. 2015;69:178-187.
10. Nakamura Y. Bluff-body aerodynamics and turbulence. J Wind Eng Ind Aerodyn. 1993;49(1):65-78.
11. Greenway ME. An analytical approach to wind velocity gust factors. J Wind Eng Ind Aerodyn. 1979;5(1):61-91.
12. Jain A, Jones NP, Scanlan RH. Coupled flutter and buffeting analysis of long-span bridges. Journal of Structural Engineering. 1996;122(7):716-725.
13. Holdø AE, Houghton EL, Bhinder FS. Some effects due to variations in turbulence integral length scales on the pressure distribution on wind-tunnel models of low-rise buildings. J Wind Eng Ind Aerodyn. 1982;10(1):103-115.
14. Metzger M, McKeon BJ, Holmes H. The near-neutral atmospheric surface layer: turbulence and non-stationarity. Philos Trans R Soc. 2007;365(1852):859-876.
15. Plate EJ. Aerodynamic Characteristics of Atmospheric Boundary Layers. Springfield, Virginia, USA: US Atomic Energy Commission; 1974.
16. Yang H, Bo T. Scaling of Wall-Normal Turbulence Intensity and Vertical Eddy Structures in the Atmospheric Surface Layer. Boundary-Layer Meteorology. 2018;166(2):199-216.
17. Mikkelsen T, Larsen SE, Jørgensen HE, et al. Scaling of turbulence spectra measured in strong shear flow near the Earth’s surface. Physica Scripta. 2017;92(12):124002.
18. Wilson J. Statistics of the Wind-Speed Difference Between Points with Cross-Wind Separation. Boundary-Layer Meteorology. 2013;146(1):149-160.
19. Wilson J. Monin-Obukhov functions for standard deviations of velocity. Boundary-Layer Meteorology. 2008;129(3):353-369.
20. Charuchittipan D, Wilson J. Turbulent kinetic energy dissipation in the surface layer. Boundary-Layer Meteorology. 2009;132(2):193-204.
21. McNaughton K, Clement R, Moncrieff J. Scaling properties of velocity and temperature spectra above the surface friction layer in a convective atmospheric boundary layer. Nonlin Process Geophys. 2007;14(3):257-271.

22. Teunissen HW. Structure of mean winds and turbulence in the planetary boundary layer over rural terrain. Boundary-Layer Meteorology. 1980;19(2):187-221.
23. Counihan J. Adiabatic atmospheric boundary layers: a review and analysis of data from the period 1880–1972. Atmospheric Environment. 1975;9(10):871-905.
24. Flay RGJ, Stevenson DC. Integral length scales in strong winds below 20 m. J Wind Eng Ind Aerodyn. 1988;28(1):21-30.
25. Panofsky HA, Tennekes H, Lenschow DH, et al. The characteristics of turbulent velocity components in the surface layer under convective conditions. Boundary-Layer Meteorol. 1977;11(3):355-361.
26. Panofsky HA, Larko D, Lipschutz R, et al. Spectra of velocity components over complex terrain. Q J R Meteorol Soc. 1982;108(455):215-230.
27. ESDU 85020. Characteristics of atmospheric turbulence near the ground, Part II: single point data for strong winds (neutral atmosphere). London: Engineering Sciences Data Unit.
28. ESDU 86010. Characteristics of atmospheric turbulence near the ground, Part III: Variations in space and time for strong winds (neutral atmosphere). London, UK: Engineering Sciences Data Unit.
29. Cook NJ. The Deaves and Harris ABL model applied to heterogeneous terrain. J Wind Eng Ind Aerodyn. 1997;66(3):197-214.
30. Xu YL. Wind Effects on Cable-Supported Bridges. Singapore: John Wiley & Sons; 2013.
31. American Society of Civil Engineers. Minimum design loads for buildings and other structures. Reston, Virginia, USA: American Society of Civil Engineers. Standard No.: 087262904X.
32. AS/NZS 1170.2. Structural Design Actions - Part 2: Wind actions. Sydney: Standards Australia and Standards New Zealand; 2011. p. pp. 26-41.
33. Stull RB. An introduction to boundary layer meteorology. Vol. 13. Dordrecht, Netherlands: Kluwer Academic; 1988.
34. Högström ULF. Non-dimensional wind and temperature profiles in the atmospheric surface layer: A re-evaluation. Boundary-Layer Meteorology. 1988;42(1):55-78.
35. Kaimal JC, Finnigan JJ. Atmospheric Boundary Layer Flows: Their Structure and Measurement. New York, USA: Oxford University Press; 1994.
36. Swamy NVC, Gowda BHL, Lakshminath VR. Auto-correlation measurements and integral time scales in three-dimensional turbulent boundary layers. Applied Scientific Research. 1979;35(4):237-249.
37. Tennekes H, Lumley JL. A First Course in Turbulence. Cambridge, Massachusetts, USA: MIT press; 1972.
38. Solari G, Piccardo G. Probabilistic 3-D turbulence modeling for gust buffeting of structures. Probabilistic Engineering Mechanics. 2001;16(1):73-86.
39. Holmes JD, Kwok KCS, Ginger JD. Wind Loading Handbook for Australia and New Zealand: Background to AS/NZS 1170.2 Wind Actions. Sydney: Australasian Wind Engineering Society; 2012.
40. Marusic I, Hutchins N. Study of the log-layer structure in wall turbulence over a very large range of Reynolds number. Flow Turbul Combust. 2008;81:115-130.
41. Van den Berg GP. The sound of high winds: The effect of atmospheric stability on wind turbine sound and microphone noise. Groningen, Netherlands: Groningen University; 2006.
42. Stull RB. The Atmospheric Boundary Layer. Vancouver, Canada: University of British Columbia; 2005.

43. Kunkel GJ, Marusic I. Study of the near-wall-turbulent region of the high-Reynolds-number boundary layer using an atmospheric flow. J Fluid Mech. 2006;548:375-402.
44. Hinze JO. Turbulence. Vol. 218. New York, USA: McGraw-Hill; 1975.
45. Chauhan KA. Study of canonical wall-bounded turbulent flows: Illinois Institute of Technology; 2007.
46. Salesky ST, Chamecki M, Dias NL. Estimating the random error in eddy-covariance based fluxes and other turbulence statistics: the filtering method. Boundary-layer meteorology. 2012;144(1):113-135.
47. Milbank J, Loxton B, Watkins S, et al. Replication of Atmospheric Conditions for the Purpose of Testing MAVs: MAV Flight Environment Project Final Report. Royal Melbourne Institute of Technology; 2005.
48. O'Neill PL, Nicolaides D, Honnery D, et al., editors. Autocorrelation functions and the determination of integral length with reference to experimental and numerical data. 15th Australasian Fluid Mechanics Conference The University of Sydney, Sydney, Australia; 2004.
49. Farell C, Iyengar AK. Experiments on the wind tunnel simulation of atmospheric boundary layers. J Wind Eng Ind Aerodyn. 1999;79(1):11-35.